EUROPEAN COOPERATION
IN SCIENCE
AND TECHNOLOGY

EURO-COST

CA15104 TD(19)11008
Gdańsk, Poland
September 4-6, 2019

SOURCE: Aalborg University, Denmark
Oulu University, Finland
Keysight Technologies, Finland
Huawei Technologies, China

Antenna Correlation Under Geometry-Based Stochastic Channel Models

Yilin Ji, Wei Fan, Pekka Kyösti, Jinxing Li, and Gert Frølund Pedersen

Yilin Ji
Aalborg University
Selma Lagerløfs Vej 312,
9220 Aalborg,
Denmark
Phone: + 45-99408727
Email: yilin@es.aau.dk

Antenna Correlation Under Geometry-Based Stochastic Channel Models

Yilin Ji, Wei Fan, Pekka Kyösti, Jinxing Li, and Gert Frølund Pedersen

***Abstract*—Antenna correlation is an important measure for designing multiple-input multiple-output (MIMO) antenna systems. A lower antenna correlation indicates a better MIMO performance that can be achieved with the underlying antenna systems. In the antenna design industry, it is very common to evaluate the antenna correlation with isotropic or non-isotropic (e.g. Gaussian-distributed) angular power spectrum as baselines. Channel models developed in the propagation field, such as the geometry-based stochastic channel model, can also be used to approach a more realistic results. In this paper, the analytic forms for the antenna correlation based on the channel transfer function and the angular power spectrum are derived, respectively, with their similarities and differences explained. Moreover, a numerical example is also given with a standard channel model.**

***Index Terms*—MIMO, antenna correlation, GSCM models, spread function, angular power spectrum.**

I. Introduction

Antenna correlation (also known as envelope correlation if absolute-squared) is widely used as a measure in both the antenna field and the propagation field considering multiple-input multiple-output (MIMO) communications. It shows how much the received signals at different antenna ports correlate with each other. A lower antenna correlation indicates a better performance can be expected for MIMO communications.

Without loss of generality, if we take the antenna correlation on the receive (Rx) side for example, the Rx antenna correlation can be analytically calculated with arbitrary incident angular power spectrum (APS) and Rx antenna field pattern [1]. It is very common in the antenna design industry to evaluate the antenna correlation of the devices with some simplified channel models such as APS following the isotropic or non-isotropic (e.g. Gaussian or Laplacian) distributions as baselines [2]. However, though simple to implement, those models may not be representative for real-world radio propagation. Therefore, it arises the need to evaluate the antenna correlation with more realistic channel models such as the geometry-based stochastic channel model (GSCM) developed in the propagation field and adopted in the standard [3].

The GSCM models are usually implemented through channel transfer function (CTF) which describes the input-output relation between the transmit (Tx) and the Rx ports of a communication system under a given propagation channel. Therefore, it is also natural to calculate the antenna correlation with CTF. As CTF describes the channel between the Tx and Rx ports, antenna pattern is generally embedded in CTF, whereas APS only describes the pure channel spatial characteristic with the Tx and Rx antenna radiation pattern de-embedded. Therefore, there are actually some differences between the Rx antenna correlation from APS and from CTF due to the spatial selectivity of the Tx antennas. Stronger Tx antenna spatial selectivity potentially alters the effective APS observed on the Rx side more severely, and hence leads to more severe inconsistency between the two Rx antenna correlations. Therefore, this inconsistency can be more profound for Tx operating in beamforming mode, e.g. the fifth-generation (5G) base stations.

In this paper, we go through the basics on calculating the antenna correlation from CTF and from APS, respectively. The connection between the two antenna correlations is built through the spread function. The analytic form of the antenna correlation under the GSCM model is derived explicitly. The difference between the end results of the antenna correlation from the two sources are clarified, which may show some useful insights for antenna designers on how to evaluate the antenna correlation of their specific antenna designs under the GSCM model. Finally, a numerical example is given with a standard channel model [3].

The notation used in the paper are summarized as follow: $(\cdot)^{\mathrm{T}}$, $(\cdot)^*$, $|\cdot|$, and $\odot$ are the transpose, the complex conjugate, the absolute value, and the Hadamard product operator, respectively. Moreover, $cov\{\cdot,\cdot\}$, $var\{\cdot\}$, and $\mathbb{E}\{\cdot\}$ are the covariance, variance, and expectation operator, respectively.

II. Propagation Channel Model

A. Channel Transfer Function

The propagation channel is usually modelled as the superposition of a number of paths. For a MIMO system consisting of S Tx antennas and U Rx antennas, the CTF from the sth Tx antenna to the uth Rx antenna at time t and frequency f can be expressed as [4]

$$\begin{aligned} &H_{u,s}(t,f) \\ &= \iiiint \begin{bmatrix} F_s^{\mathrm{V}}(\mathbf{\Omega}^{\mathrm{Tx}}) \\ F_s^{\mathrm{H}}(\mathbf{\Omega}^{\mathrm{Tx}}) \end{bmatrix}^{\mathrm{T}} \boldsymbol{h}(\tau,\upsilon,\mathbf{\Omega}^{\mathrm{Tx}},\mathbf{\Omega}^{\mathrm{Rx}}) \begin{bmatrix} F_u^{\mathrm{V}}(\mathbf{\Omega}^{\mathrm{Rx}}) \\ F_u^{\mathrm{H}}(\mathbf{\Omega}^{\mathrm{Rx}}) \end{bmatrix} \\ &\quad \cdot \exp(j2\pi\upsilon t) \cdot \exp(-j2\pi f\tau)\, \mathrm{d}\tau\, \mathrm{d}\upsilon\, \mathrm{d}\mathbf{\Omega}^{\mathrm{Tx}}\, \mathrm{d}\mathbf{\Omega}^{\mathrm{Rx}}, \end{aligned} \tag{1}$$

where $\tau, \upsilon, \mathbf{\Omega}^{\mathrm{Tx}}, \mathbf{\Omega}^{\mathrm{Rx}}$ are the domains of delay, Doppler frequency, direction of departure (DoD), direction of arrival

Yilin Ji, Wei Fan, and Gert Frølund Pedersen are with Antenna Propagation and Millimeter-wave Systems (APMS) section at Department of Electronic Systems, Aalborg University, Denmark. (Corresponding author: Wei Fan. Email: wfa@es.aau.dk)

Pekka Kyösti is with University of Oulu, Finland, and with Keysight Technologies Finland oy, Finland.

Jinxing Li is with Huawei Technologies Co., Ltd.

(DoA), respectively. $F_s^{\mathrm{V}}(\boldsymbol{\Omega})$ and $F_s^{\mathrm{H}}(\boldsymbol{\Omega})$ are the antenna field patterns of the sth Tx antenna at the direction $\boldsymbol{\Omega}$ for vertical polarization (V-pol) and horizontal polarization (H-pol), respectively. Similarly, $F_u^{\mathrm{V}}(\boldsymbol{\Omega})$ and $F_u^{\mathrm{H}}(\boldsymbol{\Omega})$ are those for the uth Rx antenna. The antenna field pattern is defined with a common phase center for the antenna array. The integration is conducted over the full span of the respective domains.

In (1), the matrix $\boldsymbol{h}$ is the so-called spread function, and within the context of the GSCM models it can be written as

$$\boldsymbol{h}(\tau,\upsilon,\boldsymbol{\Omega}^{\mathrm{Tx}},\boldsymbol{\Omega}^{\mathrm{Rx}}) = \sum_{m=1}^{M} \sqrt{P_m}\cdot\boldsymbol{A}\cdot\delta(\tau-\tau_m)\cdot\delta(\upsilon-\upsilon_m) \cdot\delta(\boldsymbol{\Omega}^{\mathrm{Tx}}-\boldsymbol{\Omega}_m^{\mathrm{Tx}})\cdot\delta(\boldsymbol{\Omega}^{\mathrm{Rx}}-\boldsymbol{\Omega}_m^{\mathrm{Rx}}), \quad (2)$$

where M is the number of paths, P_m is the power of the mth path, $\tau_m,\upsilon_m,\boldsymbol{\Omega}_m^{\mathrm{Tx}},\boldsymbol{\Omega}_m^{\mathrm{Rx}}$ are the parameters of the mth path in their respective domains, and $\delta(\cdot)$ is the Dirac delta function. The matrix $\boldsymbol{A}$ is the polarization matrix

$$\boldsymbol{A} = \begin{bmatrix} \exp(j\Phi_m^{\mathrm{VV}}) & \sqrt{\kappa_{1,m}^{-1}}\exp(j\Phi_m^{\mathrm{VH}}) \\ \sqrt{\kappa_{2,m}^{-1}\chi_m^{-1}}\exp(j\Phi_m^{\mathrm{HV}}) & \sqrt{\chi_m^{-1}}\exp(j\Phi_m^{\mathrm{HH}}) \end{bmatrix}, \quad (3)$$

where

- Φ_m^{VV}, Φ_m^{VH}, Φ_m^{HV}, and Φ_m^{HH} are the initial phases of the mth path of vertical-to-vertical (VV-pol), vertical-to-horizontal (VH-pol), horizontal-to-vertical (HV-pol), and horizontal-to-horizontal (HH-pol) polarizations, respectively. They are assumed independent and identically distributed (i.i.d.) random variables following the uniform distribution over $[0, 2\pi]$.
- $\kappa_{1,m}$ and $\kappa_{2,m}$ are the cross-polarization ratios (XPR) of the mth path, where $\kappa_{1,m}$ is the power ratio of VV-pol over VH-pol, and $\kappa_{2,m}$ HH-pol over HV-pol. It is usually assumed $\kappa_{1,m} = \kappa_{2,m} = \kappa_m$.
- χ_m is the co-polarization ratio (CPR) of the mth path. The CPR is defined as the power ratio of VV-pol over HH-pol.

Inserting (2) and (3) into (1) yields

$$H_{u,s}(t,f) = \sum_{m=1}^{M}\sqrt{P_m}\begin{bmatrix}F_s^{\mathrm{V}}(\boldsymbol{\Omega}_m^{\mathrm{Tx}})\\F_s^{\mathrm{H}}(\boldsymbol{\Omega}_m^{\mathrm{Tx}})\end{bmatrix}^{\mathrm{T}}\boldsymbol{\mathrm{A}}\begin{bmatrix}F_u^{\mathrm{V}}(\boldsymbol{\Omega}_m^{\mathrm{Rx}})\\F_u^{\mathrm{H}}(\boldsymbol{\Omega}_m^{\mathrm{Rx}})\end{bmatrix} \cdot\exp(j2\pi\upsilon_m t)\cdot\exp(-j2\pi f\tau_m). \quad (4)$$

For brevity, in the following we abbreviate the notation as: $H_{u,s}(t,f) = H_{u,s}$; $F_s^{\mathrm{V}}(\boldsymbol{\Omega}_m^{\mathrm{Tx}}) = F_{s,m}^{\mathrm{V}}$; $F_s^{\mathrm{H}}(\boldsymbol{\Omega}_m^{\mathrm{Tx}}) = F_{s,m}^{\mathrm{H}}$; $F_u^{\mathrm{V}}(\boldsymbol{\Omega}_m^{\mathrm{Rx}}) = F_{u,m}^{\mathrm{V}}$; $F_u^{\mathrm{H}}(\boldsymbol{\Omega}_m^{\mathrm{Rx}}) = F_{u,m,}^{\mathrm{H}}$.

B. Angular Power Spectrum Derived from Spread Function

The joint delay-Doppler-DoD-DoA power spectrum can be derived from the spread function as [4]

$$\boldsymbol{P}(\tau,\upsilon,\boldsymbol{\Omega}^{\mathrm{Tx}},\boldsymbol{\Omega}^{\mathrm{Rx}}) = \mathbb{E}\left\{\boldsymbol{h}(\tau,\upsilon,\boldsymbol{\Omega}^{\mathrm{Tx}},\boldsymbol{\Omega}^{\mathrm{Rx}})\odot\boldsymbol{h}(\tau,\upsilon,\boldsymbol{\Omega}^{\mathrm{Tx}},\boldsymbol{\Omega}^{\mathrm{Rx}})^*\right\}. \quad (5)$$

Inserting (2) into (5), and defining $|\delta(x)|^2 \doteq \delta(x)$ with x being the dummy variable, we can obtain

$$\boldsymbol{P}(\tau,\upsilon,\boldsymbol{\Omega}^{\mathrm{Tx}},\boldsymbol{\Omega}^{\mathrm{Rx}}) = \sum_{m=1}^{M} P_m\cdot\overline{\boldsymbol{A}^2}\cdot\delta(\tau-\tau_m)\cdot\delta(\upsilon-\upsilon_m) \cdot\delta(\boldsymbol{\Omega}^{\mathrm{Tx}}-\boldsymbol{\Omega}_m^{\mathrm{Tx}})\cdot\delta(\boldsymbol{\Omega}^{\mathrm{Rx}}-\boldsymbol{\Omega}_m^{\mathrm{Rx}}), \quad (6)$$

where

$$\overline{\boldsymbol{A}^2} = \mathbb{E}\left\{\boldsymbol{A}\odot\boldsymbol{A}^*\right\} = \begin{bmatrix}1 & \kappa_m^{-1}\\ \kappa_m^{-1}\chi_m^{-1} & \chi_m^{-1}\end{bmatrix}, \quad (7)$$

using the i.i.d. property of the initial phases of the paths.

Conventionally, power spectrum is considered as a property of propagation channels, and it is independent on the antennas used on both the Tx and the Rx. In other words, the antenna pattern is de-embedded from the channel. It follows that the power spectrum in one (either marginal or joint) domain can be obtained by integrating the joint power spectrum with higher dimensions over the remaining domains [4]. Therefore, the joint DoD-DoA power spectrum can be derived as

$$\begin{aligned}\boldsymbol{P}(\boldsymbol{\Omega}^{\mathrm{Tx}},\boldsymbol{\Omega}^{\mathrm{Rx}}) &= \iint\boldsymbol{P}(\tau,\upsilon,\boldsymbol{\Omega}^{\mathrm{Tx}},\boldsymbol{\Omega}^{\mathrm{Rx}})\,\mathrm{d}\tau\,\mathrm{d}\upsilon\\ &= \sum_{m=1}^{M} P_m\cdot\overline{\boldsymbol{A}^2}\cdot\delta(\boldsymbol{\Omega}^{\mathrm{Tx}}-\boldsymbol{\Omega}_m^{\mathrm{Tx}})\cdot\delta(\boldsymbol{\Omega}^{\mathrm{Rx}}-\boldsymbol{\Omega}_m^{\mathrm{Rx}}),\end{aligned} \quad (8)$$

which is a 2×2 matrix with the polarization relation between the Tx and the Rx in $\overline{\boldsymbol{A}^2}$.

The power spectrum in the DoA domain can be further derived in a similar way as

$$\boldsymbol{P}(\boldsymbol{\Omega}^{\mathrm{Rx}}) = \int\begin{bmatrix}1\\1\end{bmatrix}^{\mathrm{T}}\boldsymbol{P}(\boldsymbol{\Omega}^{\mathrm{Tx}},\boldsymbol{\Omega}^{\mathrm{Rx}})\,\mathrm{d}\boldsymbol{\Omega}^{\mathrm{Tx}}, \quad (9)$$

where the vector of ones describes the antenna de-embedding assumption, and merges the V-pol and H-pol contribution from the Tx side. Inserting (8) into (9), $\boldsymbol{P}(\boldsymbol{\Omega}^{\mathrm{Rx}})$ can be explicitly expressed in both polarizations as

$$\boldsymbol{P}(\boldsymbol{\Omega}^{\mathrm{Rx}}) = \begin{bmatrix}P^{\mathrm{V}}(\boldsymbol{\Omega}^{\mathrm{Rx}})\\P^{\mathrm{H}}(\boldsymbol{\Omega}^{\mathrm{Rx}})\end{bmatrix}^{\mathrm{T}}, \quad (10)$$

where

$$P^{\mathrm{V}}(\boldsymbol{\Omega}^{\mathrm{Rx}}) = \sum_{m=1}^{M} P_m\cdot(1+\kappa_m^{-1}\chi_m^{-1})\cdot\delta(\boldsymbol{\Omega}^{\mathrm{Rx}}-\boldsymbol{\Omega}_m^{\mathrm{Rx}}), \quad (11a)$$

$$P^{\mathrm{H}}(\boldsymbol{\Omega}^{\mathrm{Rx}}) = \sum_{m=1}^{M} P_m\cdot(\kappa_m^{-1}+\chi_m^{-1})\cdot\delta(\boldsymbol{\Omega}^{\mathrm{Rx}}-\boldsymbol{\Omega}_m^{\mathrm{Rx}}). \quad (11b)$$

In many GSCM models [3], [5], the CPR $\chi_m = 1$ is often assumed which leads to $P^{\mathrm{V}}(\boldsymbol{\Omega}^{\mathrm{Rx}}) = P^{\mathrm{H}}(\boldsymbol{\Omega}^{\mathrm{Rx}})$.

III. Antenna Correlation

A. Antenna Correlation from Channel Transfer Function

The antenna correlation between two Rx antenna u_1 and u_2 can be calculated as

$$\rho_{u_1,u_2}^{\mathrm{CTF}} = \frac{cov\{H_{u_1,s},H_{u_2,s}\}}{\sqrt{var\{H_{u_1,s}\}}\cdot\sqrt{var\{H_{u_2,s}\}}}. \quad (12)$$

Inserting (3) and (4) into (12), and using the i.i.d. property of the initial phases of the paths [6], it yields

$$\rho^{\text{CTF}}_{u_1,u_2} = \frac{\beta_{u_1,u_2}}{\sqrt{\beta_{u_1}} \cdot \sqrt{\beta_{u_2}}}, \tag{13}$$

where

$$\begin{aligned}\beta_{u_1,u_2} &= \sum_{m=1}^{M} \Big\{ P_m(|F^{\text{V}}_{s,m}|^2 + \kappa_m^{-1}\chi_m^{-1}|F^{\text{H}}_{s,m}|^2) \cdot F^{\text{V}}_{u_1,m} \cdot F^{\text{V}*}_{u_2,m} \\ &\quad + P_m(\kappa_m^{-1}|F^{\text{V}}_{s,m}|^2 + \chi_m^{-1}|F^{\text{H}}_{s,m}|^2) \cdot F^{\text{H}}_{u_1,m} \cdot F^{\text{H}*}_{u_2,m} \Big\}, \end{aligned} \tag{14a}$$

$$\begin{aligned}\beta_{u} &= \sum_{m=1}^{M} \Big\{ P_m(|F^{\text{V}}_{s,m}|^2 + \kappa_m^{-1}\chi_m^{-1}|F^{\text{H}}_{s,m}|^2) \cdot |F^{\text{V}}_{u,m}|^2 \\ &\quad + P_m(\kappa_m^{-1}|F^{\text{V}}_{s,m}|^2 + \chi_m^{-1}|F^{\text{H}}_{s,m}|^2) \cdot |F^{\text{H}}_{u,m}|^2 \Big\}. \end{aligned} \tag{14b}$$

B. Antenna Correlation from Angular Power Spectrum

The antenna correlation between two Rx antennas, u_1 and u_2, can also be calculated as [1] (c.f. (13))

$$\rho^{\text{APS}}_{u_1,u_2} = \frac{\gamma_{u_1,u_2}}{\sqrt{\gamma_{u_1}} \cdot \sqrt{\gamma_{u_2}}}, \tag{15}$$

where

$$\begin{aligned}\gamma_{u_1,u_2} &= \int \Big\{ \eta \cdot p^{\text{V}}(\boldsymbol{\Omega}^{\text{Rx}}) \cdot F^{\text{V}}_{u_1}(\boldsymbol{\Omega}^{\text{Rx}}) \cdot F^{\text{V}}_{u_2}(\boldsymbol{\Omega}^{\text{Rx}})^* \\ &\quad + p^{\text{H}}(\boldsymbol{\Omega}^{\text{Rx}}) \cdot F^{\text{H}}_{u_1}(\boldsymbol{\Omega}^{\text{Rx}}) \cdot F^{\text{H}}_{u_2}(\boldsymbol{\Omega}^{\text{Rx}})^* \Big\} \, \mathrm{d}\boldsymbol{\Omega}^{\text{Rx}}, \end{aligned} \tag{16a}$$

$$\begin{aligned}\gamma_{u} &= \int \Big\{ \eta \cdot p^{\text{V}}(\boldsymbol{\Omega}^{\text{Rx}}) \cdot |F^{\text{V}}_{u}(\boldsymbol{\Omega}^{\text{Rx}})|^2 \\ &\quad + p^{\text{H}}(\boldsymbol{\Omega}^{\text{Rx}}) \cdot |F^{\text{H}}_{u}(\boldsymbol{\Omega}^{\text{Rx}})|^2 \Big\} \, \mathrm{d}\boldsymbol{\Omega}^{\text{Rx}}, \end{aligned} \tag{16b}$$

with $p^{\text{V}}(\boldsymbol{\Omega}^{\text{Rx}})$ and $p^{\text{H}}(\boldsymbol{\Omega}^{\text{Rx}})$ being the normalized APS, i.e. $\int p^{\text{V}}(\boldsymbol{\Omega}^{\text{Rx}}) \, \mathrm{d}\boldsymbol{\Omega}^{\text{Rx}} = \int p^{\text{H}}(\boldsymbol{\Omega}^{\text{Rx}}) \, \mathrm{d}\boldsymbol{\Omega}^{\text{Rx}} = 1$, in the DoA domain for V-pol and H-pol, respectively. The term η is the so-called V/H ratio [3], and is defined as the ratio of the total power of the incident signal of the V-pol over that of the H-pol.

It must be noted that in the literature the V/H ratio is often termed also as XPR which is sometimes confusing to that defined in the GSCM model as described in Section II-A. Therefore, additional care shall be taken for those values in practice for calculation.

The normalized APS for both polarizations can be obtained with (11) as

$$p^{\text{V}}(\boldsymbol{\Omega}^{\text{Rx}}) = \frac{P^{\text{V}}(\boldsymbol{\Omega}^{\text{Rx}})}{P^{\text{V}}_{\text{tot}}}, \tag{17a}$$

$$p^{\text{H}}(\boldsymbol{\Omega}^{\text{Rx}}) = \frac{P^{\text{H}}(\boldsymbol{\Omega}^{\text{Rx}})}{P^{\text{H}}_{\text{tot}}}, \tag{17b}$$

with

$$P^{\text{V}}_{\text{tot}} = \sum_{m=1}^{M} P_m(1 + \kappa_m^{-1}\chi_m^{-1}), \tag{18a}$$

$$P^{\text{H}}_{\text{tot}} = \sum_{m=1}^{M} P_m(\kappa_m^{-1} + \chi_m^{-1}), \tag{18b}$$

being the total incident power for both polarizations. In addition, the V/H ratio η can be obtained as

$$\eta = \frac{P^{\text{V}}_{\text{tot}}}{P^{\text{H}}_{\text{tot}}}. \tag{19}$$

Equation (19) also indicates the V/H ratio η can be uniquely determined from the XPR κ_m and CPR χ_m but not vice versa.

Inserting (17), (18), and (19) into (16) and with some equation manipulation, we can obtain the antenna correlation $\rho^{\text{APS}}_{u_1,u_2}$ under the same channel model as for $\rho^{\text{CTF}}_{u_1,u_2}$ as

$$\begin{aligned}\gamma_{u_1,u_2} &= \sum_{m=1}^{M} \Big\{ P_m(1 + \kappa_m^{-1}\chi_m^{-1}) \cdot F^{\text{V}}_{u_1,m} \cdot F^{\text{V}*}_{u_2,m} \\ &\quad + P_m(\kappa_m^{-1} + \chi_m^{-1}) \cdot F^{\text{H}}_{u_1,m} \cdot F^{\text{H}*}_{u_2,m} \Big\}, \end{aligned} \tag{20a}$$

$$\begin{aligned}\gamma_{u} &= \sum_{m=1}^{M} \Big\{ P_m(1 + \kappa_m^{-1}\chi_m^{-1}) \cdot |F^{\text{V}}_{u,m}|^2 \\ &\quad + P_m(\kappa_m^{-1} + \chi_m^{-1}) \cdot |F^{\text{H}}_{u,m}|^2 \Big\}. \end{aligned} \tag{20b}$$

C. Relation Between the Two Antenna Correlations

By comparing (14) and (20), we can find that the antenna correlation $\rho^{\text{CTF}}_{u_1,u_2}$ and $\rho^{\text{APS}}_{u_1,u_2}$ are only different by the missing terms $|F^{\text{V}}_{s,m}|^2$ and $|F^{\text{H}}_{s,m}|^2$ in (20). Actually, this difference is caused by the antenna de-embedding assumption for the APS $\boldsymbol{P}(\boldsymbol{\Omega}^{\text{Rx}})$ given in (9).

Since the CTF describes the input-output relation between the Tx antenna ports and the Rx antenna ports, antenna pattern is not de-embedded from the CTF in the general form (1). Therefore, the power spectrum in the DoA domain for the CTF case incorporated with the Tx antenna pattern can be alternatively formulated as (c.f. (9))

$$\widetilde{\boldsymbol{P}}(\boldsymbol{\Omega}^{\text{Rx}}) = \int \begin{bmatrix} |F^{\text{V}}_{s}(\boldsymbol{\Omega}^{\text{Tx}})|^2 \\ |F^{\text{H}}_{s}(\boldsymbol{\Omega}^{\text{Tx}})|^2 \end{bmatrix}^{\text{T}} \boldsymbol{P}(\boldsymbol{\Omega}^{\text{Tx}}, \boldsymbol{\Omega}^{\text{Rx}}) \, \mathrm{d}\boldsymbol{\Omega}^{\text{Tx}}. \tag{21}$$

If we derive the antenna correlation $\rho^{\text{APS}}_{u_1,u_2}$ with respect to $\widetilde{\boldsymbol{P}}(\boldsymbol{\Omega}^{\text{Rx}})$ in the same way as in Section III-B, and denote that as $\widetilde{\rho}^{\text{APS}}_{u_1,u_2}$, it is very straightforward to find

$$\widetilde{\rho}^{\text{APS}}_{u_1,u_2} = \rho^{\text{CTF}}_{u_1,u_2}. \tag{22}$$

Alternatively, we can also consider $\rho^{\text{APS}}_{u_1,u_2}$ as a special case of $\rho^{\text{CTF}}_{u_1,u_2}$ with $|F^{\text{V}}_{s}(\boldsymbol{\Omega}^{\text{Tx}})|^2 = |F^{\text{H}}_{s}(\boldsymbol{\Omega}^{\text{Tx}})|^2 = 1$.

Another interpretation of the difference between the two antenna correlations caused by the antenna de-embedding assumption is that $\rho^{\text{APS}}_{u_1,u_2}$ is only dependent on the marginal $\boldsymbol{P}(\boldsymbol{\Omega}^{\text{Rx}})$, whereas $\rho^{\text{CTF}}_{u_1,u_2}$ is dependent on the joint $\boldsymbol{P}(\boldsymbol{\Omega}^{\text{Tx}}, \boldsymbol{\Omega}^{\text{Rx}})$ due to the spatial selectivity of the Tx antenna pattern. More intuitively, one example can be made by changing the pairing order between $\boldsymbol{\Omega}^{\text{Tx}}_{m}$ and $\boldsymbol{\Omega}^{\text{Rx}}_{m'}$ with $m, m' \in [1, M]$ for the channel. Different pairing order results in different joint $\boldsymbol{P}(\boldsymbol{\Omega}^{\text{Tx}}, \boldsymbol{\Omega}^{\text{Rx}})$, while the marginal $\boldsymbol{P}(\boldsymbol{\Omega}^{\text{Rx}})$ remains the same. It follows that $\rho^{\text{APS}}_{u_1,u_2}$ remains unchanged, while $\rho^{\text{CTF}}_{u_1,u_2}$ changes accordingly due to the spatial selectivity introduced by the Tx antenna pattern as shown in (21).

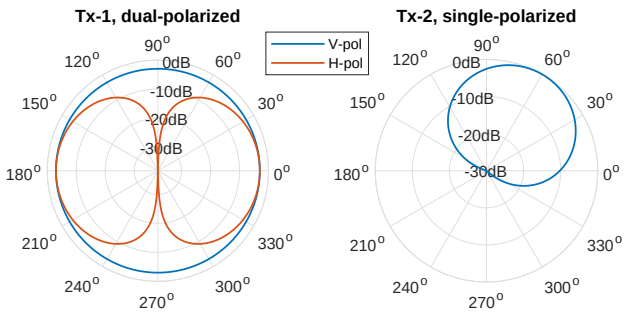

Fig. 1. The azimuth antenna pattern of (Tx-1) the 45° slanted ideal dipole [3], and (Tx-2) the V-pol dipole with 65° HPBW and boresight at 60° [5].

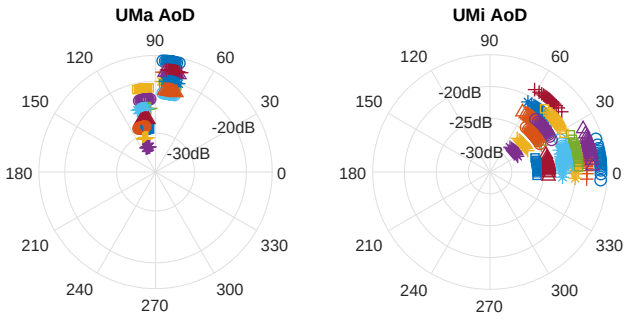

Fig. 2. The APS in the azimuth angle of departure (AoD) domain for (a) the SCME UMa scenario and (b) the SCME UMi scenario [3]. Colors and markers differ the 18 clusters and each cluster are modelled with 20 subpaths (denoted as scatterers).

IV. Numerical Examples

In this section, we take the SCME Urban Macro-cell (UMa) and Urban Micro-cell (UMi) channel model as the reference channels, and three configurations for the Tx antennas, to demonstrate the difference of the two antenna correlations. Tx config-0 (Tx-0) is the case where the Tx antennas are de-embedded; Tx config-1 (Tx-1) is a 45° slanted ideal dipole with isotropic gain; and Tx config-2 (Tx-2) is a V-pol dipole with 65° half-power beam width (HPBW) and boresight at 60°. The model for the channels and the antennas can be found in the standards [3], [5], and the corresponding Tx antenna pattern and APS in the azimuth plane are shown in Fig. 1 and Fig. 2, respectively.

The V/H ratio η is calculated from $\widetilde{\boldsymbol{P}}(\boldsymbol{\Omega}^{\mathrm{Rx}})$ with the three Tx configurations. The resulting values are shown in Table I for both the UMa and UMi scenarios with the input parameters XPR $\kappa_m = 9\,\mathrm{dB}$ and CPR $\chi_m = 0\,\mathrm{dB}$ taken from the SCME model. The difference between the values of η from different Tx configurations is significant. More specifically, the large V/H ratio for Tx-1 under the UMa scenario is caused by the polarization discrimination around 90° between the V-pol and H-pol Tx antenna pattern, where the AoDs of the paths happen to be located. When the Tx antenna is only V-pol as for Tx-2, the V/H ratio equals the XPR.

Further, the antenna correlation is calculated with isotropic antennas on the Rx side and shown in Fig. 3. The antenna spacing between the Rx antennas is swept from 0 to 2λ (wavelength), and the broadside of the two Rx antennas is aligned to 0° in the azimuth plane. The AoDs and the AoAs

TABLE I
The Effect of Tx Antenna Pattern on the Resulting V/H Ratio.

	SCME UMa			SCME UMi		
Tx Configs	κ_m	χ_m	η	κ_m	χ_m	η
Tx-0	9 dB	0 dB	0 dB	9 dB	0 dB	0 dB
Tx-1	9 dB	0 dB	8.14 dB	9 dB	0 dB	0.74 dB
Tx-2	9 dB	0 dB	9 dB	9 dB	0 dB	9 dB

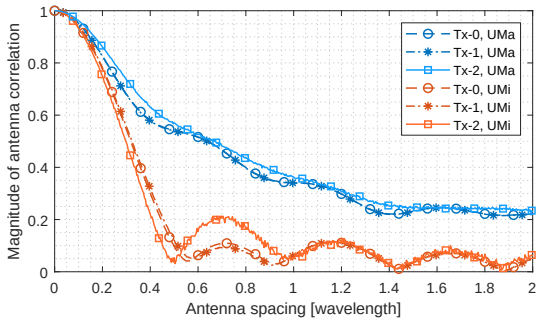

Fig. 3. The magnitude of the antenna correlation $\rho^{\mathrm{CTF}}_{u_1,u_2}$ against antenna spacing with the three Tx configurations under the UMa and the UMi channel. Note that $\rho^{\mathrm{CTF}}_{u_1,u_2}$ with Tx-0 is equivalent to $\rho^{\mathrm{APS}}_{u_1,u_2}$.

of the 20 subpaths of each cluster are first paired up randomly, and then the resulting pairing order is fixed throughout the simulation to have a fixed joint AoD-AoA power spectrum for a fair comparison of $\rho^{\mathrm{CTF}}_{u_1,u_2}$ with different Tx configurations. Note that $\rho^{\mathrm{CTF}}_{u_1,u_2}$ with Tx-0 is equivalent to $\rho^{\mathrm{APS}}_{u_1,u_2}$.

We can see that difference between $\rho^{\mathrm{CTF}}_{u_1,u_2}$ and $\rho^{\mathrm{APS}}_{u_1,u_2}$ is more significant with Tx-2 than with Tx-1 for both scenarios. The reason is that the directional antenna pattern of Tx-2 alters $\widetilde{\boldsymbol{P}}(\boldsymbol{\Omega}^{\mathrm{Rx}})$ more severely than Tx-1 does. Moreover, the difference is more significant under the UMi scenario than under the UMa scenario for the same Tx configuration. This is because the larger AoD spread under the UMi scenario introduces more variation from the Tx antenna pattern to $\widetilde{\boldsymbol{P}}(\boldsymbol{\Omega}^{\mathrm{Rx}})$ compared to the UMa scenario. Therefore, we can expect that a more noticeable difference between $\rho^{\mathrm{CTF}}_{u_1,u_2}$ and $\rho^{\mathrm{APS}}_{u_1,u_2}$ may occur if either the AoD spread of a given channel is larger or the Tx antenna pattern is more directional.

V. Conclusion

In this paper, we derived the analytic forms for the antenna correlation based on the CTF and the APS, respectively. The relation between the antenna correlation from the two sources is described with the spread function. It is shown explicitly in the derivation that the difference between them is caused by the antenna de-embedding assumption made for the APS, which is not generally assumed for the CTF. It is also pointed out that the two antenna correlations can be equivalent if the same assumption is made for the CTF.

The two antenna correlations and the V/H ratio are calculated with the SCME UMa and UMi channel model as an example, which numerically shows the effect of the spatial selectivity of the Tx antennas on the results.

REFERENCES

[1] C. A. Balanis, *Antenna Theory: Analysis and Design*. John Wiley & Sons, 2005.

[2] I. Szini, B. Yanakiev, and G. F. Pedersen, "MIMO reference antennas performance in anisotropic channel environments," *IEEE Transactions on Antennas and Propagation*, vol. 62, no. 6, pp. 3270–3280, 2014.

[3] 3GPP, "Verification of radiated multi-antenna reception performance of User Equipment (UE)," Technical Specification Group Radio Access Network, Tech. Rep. 3GPP TR 37.977 V14.3.0, 2017.

[4] B. H. Fleury, "First- and second-order characterization of direction dispersion and space selectivity in the radio channel," *IEEE Transactions on Information Theory*, vol. 46, no. 6, pp. 2027–2044, 2000.

[5] 3GPP, "Study on channel model for frequencies from 0.5 to 100 GHz," Tech. Rep. 3GPP TR 38.901 V14.0.0, 2017.

[6] P. Bello, "Characterization of Randomly Time-Variant Linear Channels," *IEEE Transactions on Communications Systems*, vol. 11, no. 4, pp. 360–393, 1963.